

Dual-directional effect of vinorelbine combined with cisplatin or fluorouracil on tumor growth and metastasis in metronomic chemotherapy in breast cancer

HUA LIU, MIN LI, YANLAN LIN, HUINING YOU, JIANRONG KOU and WEIYI FENG

Department of Pharmacy, The First Affiliated Hospital of Xi'an Jiaotong University, Xi'an, Shaanxi 710061, P.R. China

Received June 10, 2023; Accepted November 10, 2023

DOI: 10.3892/ijo.2023.5601

Abstract. Metronomic chemotherapy (MCT) regimens may be associated with risks to the patient due to the ambiguity surrounding low dosages and schedules. In the present study, metronomic regimens of vinorelbine (NVB) combined with cisplatin (CDDP) or fluorouracil (5-FU) were chosen to study the dose-response associations with tumor growth and metastasis, along with the underlying mechanisms in angiogenesis, apoptosis and tumor immunity, using experimental techniques such as immunofluorescence, immunohistochemistry, western blotting and flow cytometry. The results demonstrated a dual-directional pharmacological action of promoting and suppressing tumor growth or metastasis in BALB/c mice bearing a 4T1 tumor at certain low and high doses of the drugs. Low doses of NVB combined with CDDP or 5-FU accelerated tumor growth by enhancing angiogenesis, increasing the expression of angiogenic proteins, NF- κ B and osteopontin in tumor tissues, and inducing the accumulation of myeloid-derived suppressor cells and macrophages. By contrast, higher doses inhibited tumor growth by suppressing these effects. Notably, the upregulation of apoptotic proteins was observed after low- and high-dose treatments. Furthermore, at low concentrations, NVB combined with CDDP or 5-FU stimulated certain functions of endothelial and tumor cells, including migration and invasion, whereas at higher concentrations they suppressed proliferation and induced apoptosis. Therefore, the results of the present study suggested the potential risks of metronomic combination chemotherapy by demonstrating that, at certain low doses, tumor growth or metastasis was promoted, and emphasized the existence of an effective dose interval that changes with different drug combinations. However, further studies are needed before a specific metronomic combination regimen can be administered clinically for cancer treatment.

Introduction

In conventional chemotherapy, antineoplastic drugs are administered at a maximum tolerated dose (MTD), derived from the maximum survivable dose or minimum lethal dose, with the aim of eliminating as many proliferative tumor cells as possible (1). Accumulating evidence has indicated that the heterogeneity of tumor tissues can result in tumor cells that have different responses to the same chemotherapeutic regimen, indicating that treatment regimens should be based upon a combination of antineoplastic agents (2,3). Moreover, the current combinations of effective MTD regimens are still falling short of expectations for disease control and/or regression, frequently due to severe toxicity. There have been significant efforts to identify the optimal strategy for achieving disease control while reducing toxicity, as drug doses and schedules were found to be the determinants of chemotherapeutic efficacy (4).

Metronomic chemotherapy (MCT) involves the continuous administration of antineoplastic drugs at relatively low, effective, minimally toxic doses and without extended drug-free intervals (5). The mild toxicity of MCT may enable more effective and tolerable chemotherapy combinations, increasing the selectivity of therapeutic strategies for cancer (6,7). The purpose of combining low-dose antineoplastic drugs with different modes of action is to achieve a synergy to yield a sufficient antitumor efficacy with lower doses, and to reduce the incidence and intensity of side effects. Nevertheless, determining the optimal metronomic combination regimen has been challenging due to low dosages and drug-free intervals covering numerous possible combinations. There have been some attempts to develop metronomic combination regimens, but they were empirical in terms of determining the appropriate dosage and interval for administering antineoplastic agents due to the lack of a specific definition of MCT and standardized guidance (8,9). Furthermore, emerging evidence has indicated that low-dose antineoplastic agents, such as gemcitabine and cyclophosphamide, may promote tumor growth or metastasis, suggesting a potential risk associated with the empirical administration of chemotherapy drugs in MCT (10,11). Therefore, metronomic combination chemotherapy has only theoretical advantages, but presents a number of risks and challenges in clinical practice. Further research is urgently required to determine the optimal doses of

Correspondence to: Professor Weiyi Feng, Department of Pharmacy, The First Affiliated Hospital of Xi'an Jiaotong University, 277 Yanta West Road, Xi'an, Shaanxi 710061, P.R. China
E-mail: fengweiyi@xjtu.edu.cn

Key words: vinorelbine, metronomic chemotherapy, angiogenesis, apoptosis, tumor immunity

combination regimens, despite the proven efficacy and tolerability of metronomic combination chemotherapy (12,13).

Vinorelbine (NVB) is an anti-tubulin agent, and one of the most frequently used chemotherapy drugs in MCT, either in monotherapy or in combination with other drugs, including cisplatin (CDDP), fluorouracil (5-FU) and targeted agents such as tyrosine kinase inhibitors and immune checkpoint inhibitors (14,15). Although NVB-based metronomic combination therapy has yielded inconsistent clinical outcomes, the details about this inconsistency remain unclear (16,17). CDDP and 5-FU are extensively utilized chemotherapeutic drugs that have an antitumor effect on various types of cancer, such as breast and colorectal cancer, by inducing DNA lesions or obstructing DNA synthesis, respectively (18,19). In the present study, the dose-response associations and mechanisms of NVB-based combination regimens were investigated, specifically NVB + CDDP and NVB + 5-FU, both *in vivo* and *in vitro*.

Materials and methods

Chemicals. NVB (cat. no. 19990278) and CDDP (cat. no. 20040813) were provided by Jiangsu Hansoh Pharmaceutical Group Co., Ltd. 5-FU (cat. no. 31020593) was purchased from Shanghai Xudong Haipu Pharmaceutical Co., Ltd. The chemicals were prepared in 0.9% sodium chloride solution (cat. no. 19994067), which was obtained from Shanghai Baxter Medical Supplies Co., Ltd.

Cell lines. The human umbilical vein endothelial cell (HUVEC) line and the 4T1 breast cancer cell line were obtained from The Cell Bank of Type Culture Collection of The Chinese Academy of Sciences. The HUVEC line was cultured in DMEM media (Gibco; Thermo Fisher Scientific, Inc.) and the 4T1 cell line was cultured in RPMI-1640 media (Gibco; Thermo Fisher Scientific, Inc.), supplemented with 10% fetal bovine serum (Gibco; Thermo Fisher Scientific, Inc.) and 1% penicillin/streptomycin, in a culture chamber with 5% CO₂ at 37°C.

Tumor models. Animal experiments were approved by The Biomedical Ethics Committee of Xi'an Jiaotong University (Xi'an, China). Furthermore, the animal experiments were performed in accordance with the guide for the care and use of laboratory animals during the treatment period (20). Female BALB/c mice (6-8 weeks old; 18-22 g; GemPharmatech Co., Ltd.) were housed under a capacious and controlled environment with constant humidity, temperature (20-22°C) and a 12-h light cycle, as well as with unlimited access to chow and water to prevent death caused by environmental and feeding factors.

Mouse models of tumor growth or metastasis were established by injecting 1x10⁶ in 0.1 ml 4T1 tumor cells into the subcutaneous groin or tail vein of each mouse, respectively. In the present study, the experimental doses were determined based on published research and preliminary experiments (21,22). All mice were randomly grouped into the control or treatment groups (6 mice/group), and *i.p.* injected with either 0.9% sodium chloride solution (control), NVB + CDDP (0.03125/0.05, 0.0625/0.1, 0.125/0.2, 0.25/0.4, 0.5/0.8, 1/1.6 or 2/3.2 mg/kg) or NVB + 5-FU (0.0525/3.9375,

0.105/7.875, 0.21/15.75, 0.42/31.5 or 0.84/63 mg/kg) in a volume of 0.1 ml/10 g body weight, 24 h after tumor cell inoculation; this dosing regimen was repeated every other day for 2 weeks. The health and behavior of the mice and the size of the tumors were monitored daily. Notably, the diet of the animals was closely monitored due to the common gastrointestinal reactions such as nausea, vomiting and anorexia, associated with these chemotherapeutic drugs (23). The tumor burden did not exceed 5% of the initial body weight of the mouse, which is commonly considered a humane endpoint in mouse models. At the end of the study, the mice were anesthetized by intraperitoneal injection of 20% (1 g/kg) urethane solution and sacrificed by cervical dislocation. The blood, tumors and lungs of the tumor-bearing mice were collected for further examination.

Cell-counting kit-8 (CCK-8) and MTT assays. HUVEC and 4T1 cell viability was measured by CCK-8 or MTT assays. The maximal concentration (C_{max}) of NVB + CDDP or NVB + 5-FU was determined using the following formula: C_{max(NVB + CDDP)} = IC_{50(NVB)} + IC_{50(CDDP)} or C_{max(NVB + 5-FU)} = IC_{50(NVB)} + IC_{50(5-FU)}. Next, the cells were seeded at 2.5x10³ cells/well in a 96-well plate and treated with a series of concentrations of NVB + CDDP and NVB + 5-FU. The cells were incubated with CCK-8 (cat. no. AR1160; Boster Biological Technology) or MTT (cat. no. 1334MG250; BioFroxx; neoFroxx) reagent for 1 or 4 h, respectively, before measuring the absorbance using a Multimode Reader (Synergy LX; BioTek) at 450 nm for CCK-8 or 490 nm for MTT.

Cell apoptosis. Briefly, 1x10⁵ HUVECs or 4T1 tumor cells per well were seeded in a 6-well plate and harvested by centrifugation (1,000 x g, 5 min, 4°C) following treatment with antineoplastic agents. The HUVECs or 4T1 cells were treated with NVB + CDDP (0.03/88 and 3.6/1.1x10⁴ nM; 0.125/37.5 and 4/1.2x10³ nM) and NVB + 5-FU (0.1/1.4x10³ and 3.6/4.5x10⁴ nM; 0.06/5.3 nM and 4/340 nM). The harvested cells were processed using an Annexin V-PE/7-AAD Apoptosis Detection Kit (cat. no. G1512-50; Wuhan Servicebio Technology Co., Ltd.), following the manufacturer's instructions. Next, cell apoptosis was measured by Flow Cytometry (FACSCanto™ II; BD Biosciences) and analyzed by FlowJo version 10 software (FlowJo LLC).

Wound healing assay and Transwell assay. The HUVECs or 4T1 cells were treated with NVB + CDDP (0.03/88 and 3.6/1.1x10⁴ nM; 0.25/75 and 4/1.2x10³ nM) and NVB + 5-FU (0.1/1.4x10³ and 3.6/4.5x10⁴ nM; 0.03/2.7 nM and 4/340 nM) *in vitro*, respectively.

For wound healing assay, HUVECs or 4T1 cells were seeded and cultured in a 6-well plate with media supplemented with 10% FBS until 80-90% confluency was reached. The cell layer was then wounded using a 200-μl pipette tip and washed with PBS to remove the non-adherent cells. Images were captured using a light microscope (XD-202; Nanjing Jiangnan Novel Optics Co., Ltd.) with x100 magnification before and after the cells were incubated with serum-free media containing antineoplastic agents for 24 h at 37°C. The relative change of the wound area was analyzed using Image-Pro Plus software (version 6.0; Media Cybernetics, Inc.).

The Transwell assay was performed using a 24-well plate with 8- μ m pore chambers (MilliporeSigma), as previously described (24). The top chamber was precoated with Matrigel Matrix (cat. no. 354234; Corning, Inc.) for 4 h at 37°C. Next, 5×10^5 cells were suspended with serum-free media and seeded in each chamber, and complete media containing antineoplastic agents were placed in the bottom wells. After 24 h incubation, the non-invaded cells were wiped away and the invaded cells were fixed with 4% paraformaldehyde for 10 min, followed by staining with 0.1% crystal violet dye for 10 min, both at room temperature. Images were captured using a light microscope (XD-202; Nanjing Jiangnan Novel Optics Co., Ltd.) with x100 magnification.

Hematoxylin & eosin (H&E) staining, immunohistochemistry and immunofluorescence. The tissues, including tumor and lung tissues, were fixed by immersing in a 4% paraformaldehyde solution for >24 h at room temperature. After fixation, the tissues were embedded in paraffin and cut into slices (5- μ m thickness). The lung slices were deparaffinized by a xylene and ethanol series for 5-10 min and stained with hematoxylin (1-2 min) and eosin (5 min) at room temperature to analyze the tumor metastatic nodules in the lung tissues. The images were digitized using a 3D Histech Scanner System (DX12; 3DHISTECH Ltd.).

Immunohistochemical and immunofluorescence staining were conducted as previously reported (25). Briefly, the dewaxed tissue slice (treated as aforementioned) was incubated with 3% H₂O₂ to block the endogenous peroxidase activity, immersed in sodium citrate for antigen retrieval (95-100°C for 15 min) and blocked with 5% bovine serum albumin (cat. no. AR0004; Boster Biological Technology) for 30 min at 37°C. For immunohistochemistry, the slice was incubated with osteopontin (OPN; 1:1,000; cat. no. ab283656; Abcam), matrix metalloproteinase (MMP)-2 (1:1,000; cat. no. GB11130; Wuhan Servicebio Technology Co., Ltd.) and MMP-9 (1:5,000; cat. no. ab283575; Abcam) primary antibodies overnight at 4°C, incubated with a biotin conjugated IgG (cat. no. BA1003; Boster Biological Technology) secondary antibody for 30 min at 37°C, stained with DAB and then counterstained with hematoxylin for 1-2 min at room temperature. For immunofluorescence, the slice was incubated with CD31 (1:800; cat. no. GB11063-2; Wuhan Servicebio Technology Co., Ltd.), CD11b (1:1,000; cat. no. 133357; Abcam), F4/80 (1:1,000; cat. no. 300421; Abcam) and CD206 (1:400; cat. no. GB113497-100; Wuhan Servicebio Technology Co., Ltd.) primary antibodies overnight at 4°C. The slice was then incubated with Cy3 (1:1,000; cat. no. GB21303; Wuhan Servicebio Technology Co., Ltd.) or Alexa Fluor® 488 (1:1,000; cat. no. GB25303; Wuhan Servicebio Technology Co., Ltd.)-conjugated IgG for 50 min at 37°C. Finally, the slice was stained with DAPI (cat. no. AR1177; Boster Biological Technology) for 10 min at room temperature. Images were obtained using a fluorescent Zeiss Axio Imager (Carl Zeiss AG).

Western blotting. The tumor tissues were lysed with RIPA lysis buffer (cat. no. R0020; Beijing Solarbio Science & Technology Co., Ltd.) supplemented with 1% protease and 1% phosphatase inhibitors. The protein concentrations

were quantified using a BCA protein quantification kit (cat. no. G2026; Wuhan Servicebio Technology Co., Ltd.). Equal amounts of 15 μ g denatured protein per lane were then separated on 10% SDS-PAGE gels and transferred to PVDF membranes (MilliporeSigma). The membranes were immersed in 5% (w/v) non-fat milk for 2 h at room temperature to block non-specific binding and were then cut horizontally according to the different molecular weights. The cut membranes were then incubated with the following targeted primary antibodies overnight at 4°C: β -actin (1:5,000; cat. no. bs-0061R; Bioss), VEGF (1:800; cat. no. bs-0279R; Bioss), VEGFR₁ (1:1,000; cat. no. 32152; Abcam), VEGFR₂ (1:1,000; cat. no. 9698s; CST Biological Reagents Co., Ltd.), NF- κ B (1:1,000; cat. no. 8242; CST Biological Reagents Co., Ltd.), caspase-3 (1:1,000; cat. no. 9662; CST Biological Reagents Co., Ltd.), cleaved-caspase-3 (1:1,000; cat. no. 9661; CST Biological Reagents Co., Ltd.), caspase-8 (1:1,000; cat. no. 4790T; CST Biological Reagents Co., Ltd.) and cleaved-caspase-8 (1:1,000; cat. no. 8592T; CST Biological Reagents Co., Ltd.), followed by incubation with an HRP-conjugated secondary antibody (1:8,000; cat. no. BA1054; Boster Biological Technology) for 2 h at 37°C. The signal was examined using Clarity Western ECL Substrates (Bio-Rad Laboratories, Inc.) and a ChemiDoc™ XRS+ System (Bio-Rad Laboratories, Inc.). The analysis was performed using Image Lab software version 3.0 (Bio-Rad Laboratories, Inc.).

Flow cytometry. The blood collected from the tumor-bearing mice was lysed with ammonium-chloride-potassium lysis buffer (cat. no. 00-4333-57; Thermo Fisher Scientific, Inc.) and washed with pre-cooled PBS to harvest cells by centrifugation (1,000 x g, 5 min at 4°C). The cells were incubated with PE anti-mouse Ly-6G/Ly-6C (Gr1; 0.25 μ g/ μ l; cat. no. 108407; BioLegend, Inc.), FITC anti-mouse CD11b (0.25 μ g/ μ l; cat. no. 101205; BioLegend, Inc.) and APC anti-mouse Ki-67 (0.25 μ g/ μ l; cat. no. 652405; BioLegend, Inc.) antibodies for 40 min at 4°C. The positive cells were measured using a FACSCanto II Flow Cytometry System (BD Biosciences) and analyzed by FlowJo version 10 (FlowJo LLC).

Statistical analysis. Statistical analyses were performed using SPSS software (version 19.0; IBM Corp.). Data are presented as the mean \pm SD. Comparisons of two or more groups were conducted using an unpaired sample t-test or one-way ANOVA with the Bonferroni post hoc test, respectively. P<0.05 was considered to indicate a statistically significant difference.

Results

Dual-directional effect of NVB combined with CDDP or 5-FU on tumor growth and metastasis. The dose-response association of NVB combined with CDDP or 5-FU on tumor growth was evaluated using a breast cancer mouse model, which involved the subcutaneous injection of 4T1 tumor cells into the inguinal area of BALB/c mice. The tumor weight increased by 37.32, 40.09 and 54.09% (P<0.01, P<0.01 and P<0.05, respectively) following treatment with 0.03125/0.05, 0.0625/0.1 and 0.125/0.2 mg/kg NVB + CDDP, respectively, but decreased by 37.17, 45.60 and 72.20% (all P<0.01) following treatment with 0.5/0.8, 1/1.6 and 2/3.2 mg/kg NVB + CDDP,

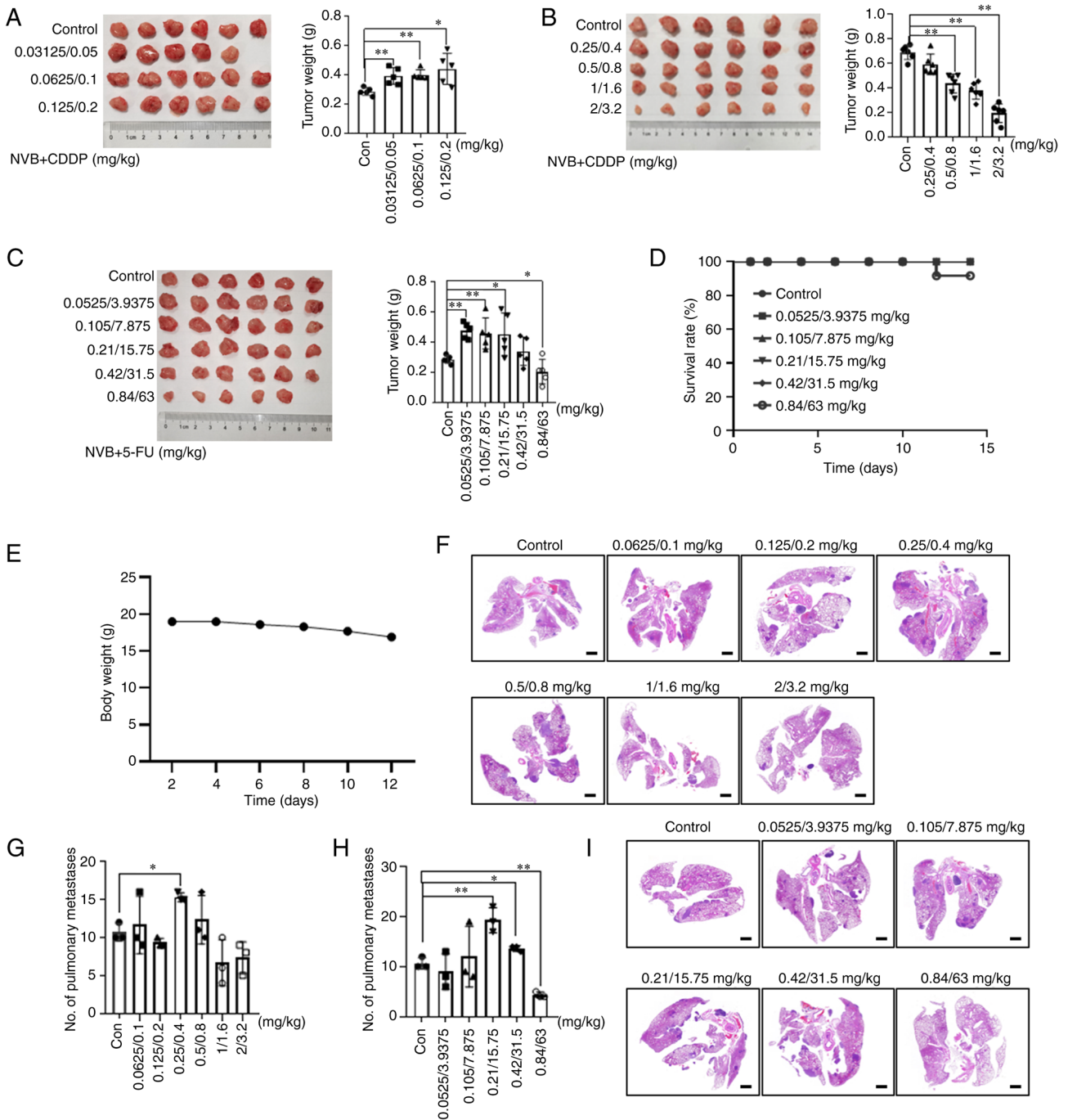


Figure 1. Effects of NVB combined with CDDP or 5-FU on tumor growth or metastasis *in vivo*. Analysis of the 4T1 tumor weight of BALB/c mice (n=6) treated with (A) low or (B) high doses of NVB + CDDP, or (C) NVB + 5-FU, administered once every other day for 2 weeks. (D) Survival curve of BALB/c mice treated with NVB + 5-FU. (E) Weight change of the mouse treated with 0.84/63 mg/kg NVB + 5-FU that died on day 12. (F) Representative images and (G) analysis of pulmonary metastatic nodules of BALB/c mice (n=3) treated with NVB + CDDP for 2 weeks, as well as the (H) analysis and (I) images of the NVB + 5-FU treatment groups. Scale bar, 1,000 μ m. *P<0.05, **P<0.01 vs. control. 5-FU, fluorouracil; CDDP, cisplatin; Con, control; NVB, vinorelbine.

respectively, compared with the control (Fig. 1A and B). One mouse in the 0.03125/0.05 mg/kg NVB + CDDP treatment group died on day 6 due to internal bleeding caused by an accident during the subcutaneous injection process. A similar result was observed in the NVB + 5-FU treatment groups (Fig. 1C), where the tumor growth increased by 67.17, 60.55 and 58.34% (P<0.01, P<0.01 and P<0.05, respectively) following treatment with 0.0525/3.9375, 0.105/7.875 and 0.21/15.75 mg/kg NVB + 5-FU, respectively, while tumor growth decreased by 28.79% (P<0.05) following

treatment with 0.84/63 mg/kg NVB + 5-FU. As shown in Fig. 1D and E, in the group receiving 0.84/63 mg/kg NVB + 5-FU, one out of the six mice exhibited weight loss (11.05%) and experienced mild diarrhea (wet and soft stool), ultimately resulting in death on day 12, possibly due to an adverse intestinal reaction (26).

Based on the aforementioned findings, the effect of NVB + CDDP or NVB + 5-FU on tumor metastasis was further investigated in a BALB/c metastasis mouse model where 4T1 cells were injected into the tail vein. The H&E results demonstrated

that the number of pulmonary metastatic nodules increased by 43.75% ($P<0.05$) following treatment with 0.25/0.4 mg/kg NVB + CDDP and increased by 81.25% ($P<0.01$) and 28.13% ($P<0.05$) following 0.21/15.75 and 0.42/31.5 mg/kg NVB + 5-FU treatment, respectively, compared with the untreated group (Fig. 1F-I). However, the number of pulmonary metastatic nodules decreased by 59.38% ($P<0.01$) following 0.84/63 mg/kg NVB + 5-FU treatment, compared with the untreated group (Fig. 1F-I). Notably, although 2/3.2 mg/kg NVB + CDDP significantly inhibited tumor growth, this dose led to an insignificant reduction in pulmonary metastases.

Collectively, these results indicated that metronomic administration of NVB + CDDP or NVB + 5-FU induced a possible dual-directional action of promoting and suppressing tumor growth and metastasis at different doses.

Dual-directional effect of NVB combined with CDDP or 5-FU on angiogenesis. To explore whether angiogenesis was involved in the dual-directional effect of metronomic combined regimens on tumor growth and metastasis, microvessel density (MVD) was observed in tumor and lung samples from the statistically significant groups by staining with a CD31 antibody, which is a surface marker of neovascular endothelial cells. The MVD significantly increased in tumor tissues by 44.05% ($P<0.05$) following treatment with 0.0625/0.1 mg/kg NVB + CDDP, compared with the control group (Fig. 2A and B). Meanwhile, the MVD increased by 145.99% ($P<0.01$) following 0.21/15.75 mg/kg NVB + 5-FU treatment and decreased by 51.77% ($P<0.05$) following 0.84/63 mg/kg NVB + 5-FU treatment, compared with the control group (Fig. 2C and D). In the lungs with metastatic tumors, 0.21/15.75 mg/kg NVB + 5-FU treatment resulted in a significant increase (132.78%) in MVD and 0.84/63 mg/kg NVB + 5-FU treatment led to a 47.60% decrease, compared with the untreated group (both $P<0.01$; Fig. 2E and F).

The expression levels of pro-angiogenic proteins, VEGF, VEGFR₁ and VEGFR₂, in the tumors were also determined by western blotting. As shown in Fig. 2G, 0.0625/0.1 mg/kg NVB + CDDP significantly increased the VEGF, VEGFR₁ and VEGFR₂ protein expression levels by 22.69, 23.90 and 37.57% (all $P<0.05$), respectively, compared with the untreated group. However, the higher dose of 2/3.2 mg/kg NVB + CDDP reduced the expression of VEGF, VEGFR₁ and VEGFR₂ by 9.08, 18.35 and 15.11%, respectively, compared with the untreated group, but the changes were not statistically significant. Similarly, the VEGF, VEGFR₁ and VEGFR₂ expression levels were significantly upregulated by 29.00, 34.32 and 23.85%, respectively ($P<0.05$, $P<0.05$ and $P<0.01$, respectively) in the 0.21/15.75 mg/kg NVB + 5-FU treatment group compared with the untreated group (Fig. 2H). However, the VEGF and VEGFR₁ expression levels were non-significantly reduced by 18.36 and 0.50%, respectively, and the VEGFR₂ expression level was significantly reduced by 32.20% ($P<0.01$), following 0.84/63 mg/kg NVB + 5-FU, compared with the untreated group (Fig. 2H).

The expression levels of angiogenesis-related proteins, MMP-2 and MMP-9, in the lung tissues were also assessed. The MMP-2 expression level was higher (38.20%; $P<0.01$) in the 0.25/0.4 mg/kg NVB + CDDP group and lower

(29.43%; $P<0.05$) in the 2/3.2 mg/kg NVB + CDDP group compared with that in the control group (Fig. 2I). In addition, 0.21/15.75 mg/kg NVB + 5-FU increased the level of MMP-9 by 64.33% ($P<0.05$), whereas 0.84/63 mg/kg NVB + 5-FU decreased the level of MMP-9 by 73.65% ($P<0.01$), compared with the untreated group (Fig. 2J).

Collectively, these findings indicated that angiogenesis likely played a role in regulating tumor growth and metastasis in the present study, and the enhancement of angiogenesis was particularly notable at low doses of combined treatment.

Promotion of apoptosis in tumors treated with low and high doses of NVB combined with CDDP or 5-FU. To observe the impact of metronomic NVB-based combination regimens on apoptosis, the expression levels of apoptosis-related proteins in tumor tissues were measured using western blotting. The levels of cleaved-caspase-3, caspase-3 and caspase-8, but not cleaved-caspase-8, were increased by 30.04, 29.22 and 45.72% ($P<0.01$, $P<0.01$ and $P<0.05$), respectively, following treatment with 0.84/63 mg/kg NVB + 5-FU, compared with the untreated group (Fig. 3A). Notably, low-dose 0.21/15.75 mg/kg NVB + 5-FU also significantly increased the expression levels of cleaved-caspase-3, cleaved-caspase-8 and caspase-8 by 53.52, 44.69 and 32.48% ($P<0.01$, $P<0.01$ and $P<0.05$), respectively, compared with the control group. Similar results were obtained in the low-dose NVB + CDDP treatment groups. 0.0625/0.1 mg/kg NVB + CDDP significantly increased the expression levels of cleaved-caspase-3, caspase-3, cleaved-caspase-8 and caspase-8 by 29.44, 35.06, 51.98 and 27.04% ($P<0.05$, $P<0.01$, $P<0.01$ and $P<0.01$), respectively, compared with the untreated group (Fig. 3B). These findings suggested that either low or high dose treatments enhanced the expression of apoptotic proteins. Meanwhile, the inhibition of tumor growth induced by high-dose treatment was related to the upregulation of apoptosis-related proteins.

Previous studies suggest that, despite its known role in tumor suppression, apoptosis may stimulate tumor growth through the participation of NF- κ B and OPN (27,28). In the present study, it was found that the expression level of NF- κ B was higher (25.45%; $P<0.05$) in the 0.0625/0.1 mg/kg NVB + CDDP group than in the control group, and lower (14.42%;) in the 2/3.2 mg/kg NVB + CDDP group, but this result was not significant (Fig. 3C). Meanwhile, 0.0625/0.1 mg/kg NVB + CDDP increased the OPN expression level by 51.39% ($P<0.01$), whereas 2/3.2 mg/kg NVB + CDDP decreased the OPN expression level by 49.52% ($P<0.05$), compared with the untreated group (Fig. 3D and E). Furthermore, the OPN expression level increased by 29.7% in the 0.21/15.75 mg/kg NVB + 5-FU group and decreased by 41.35% in the 0.84/63 mg/kg NVB + 5-FU group, compared with the untreated group (both $P<0.05$; Fig. 3F and G). These findings demonstrated that the role of apoptosis in tumor growth may be influenced by NF- κ B and OPN, at low treatment doses.

The Ki67 index, a well-recognized marker for the evaluation of cell proliferation, independently predicts the malignancy of tumors (29,30). Therefore, the effect of NVB-based combination regimens on Ki67 expression was investigated in the blood and lungs of mice with metastatic tumors. Although no significant differences were identified in the percentage of

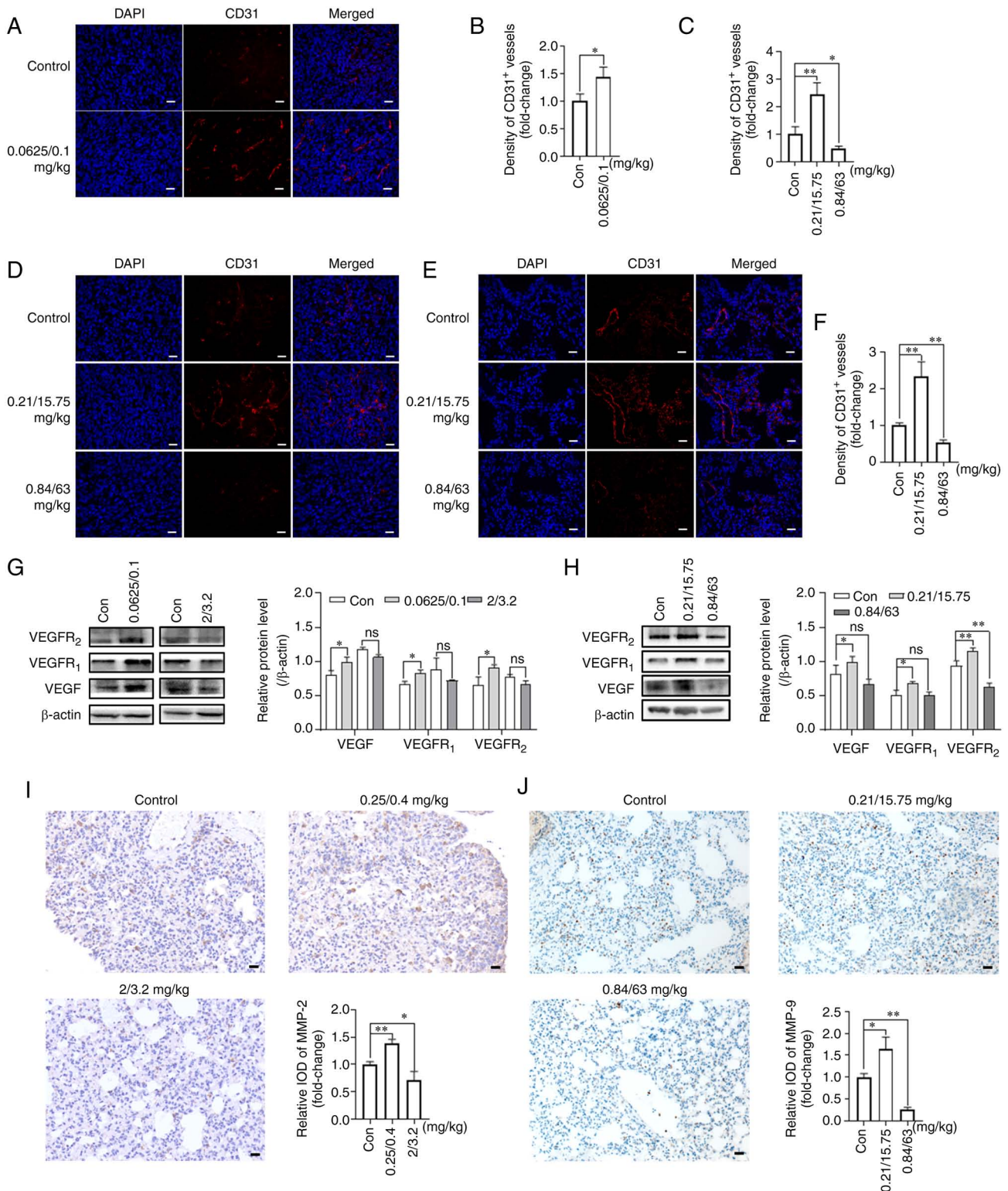


Figure 2. Effects of NVB combined with CDDP or 5-FU on angiogenesis. (A) Representative images and (B) analysis of CD31 (red) in 4T1 tumors treated with 0.0625/0.1 mg/kg NVB + CDDP using immunofluorescence. The cell nuclei were counterstained with DAPI (blue). (C) Analysis and (D) representative images of CD31 in tumors of BALB/c mice treated with NVB + 5-FU, as well as (E) images and (F) analysis of CD31 in the lungs. VEGF, VEGFR1 and VEGFR2 protein levels were detected in 4T1 tumors following treatment with (G) NVB + CDDP or (H) NVB + 5-FU using western blotting. Detection of (I) MMP-2 and (J) MMP-9 in the lungs of metastatic BALB/c mice treated with NVB + CDDP or NVB + 5-FU using immunohistochemistry. n=3. Scale bar, 20 μm. *P<0.05, **P<0.01 vs. control. 5-FU, fluorouracil; CDDP, cisplatin; Con, control; IOD, integral optical density; MMP, matrix metalloproteinase; ns, not significant; NVB, vinorelbine; ns, not significant.

Ki67+ cells in the blood of different subgroups treated with NVB + CDDP or NVB + 5-FU (Fig. 3H-K), the number of Ki67+ cells in the lungs increased following treatment with

0.21/15.75 mg/kg NVB + 5-FU but decreased following 0.84/63 mg/kg NVB + 5-FU (Fig. 3L). These results suggested that the number of Ki67+ cells in tissues may be more valuable

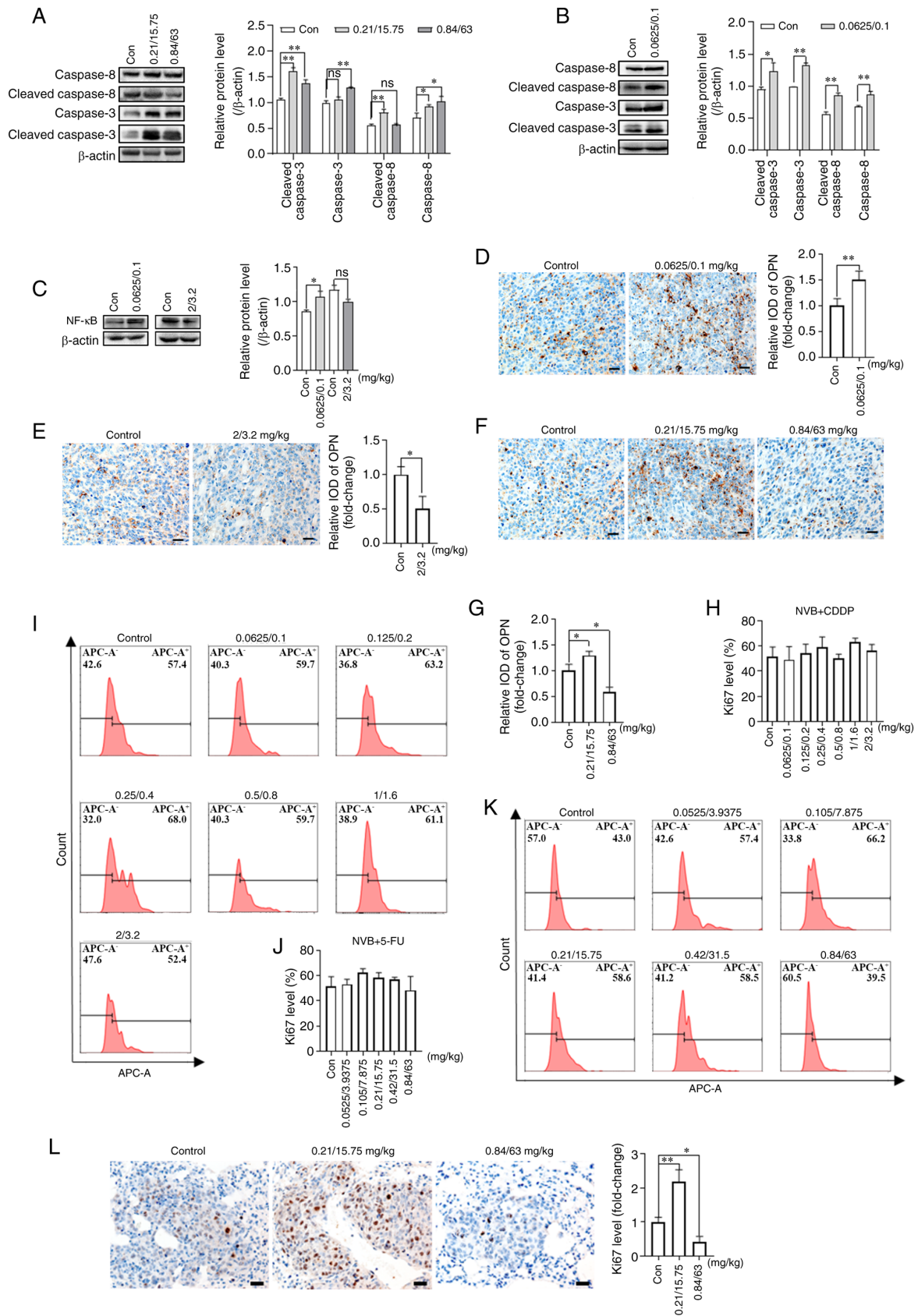


Figure 3. Effects of NVB combined with CDDP or 5-FU on apoptosis and Ki67 expression. Detection of the cleaved-caspase-3, caspase-3, cleaved-caspase-8 and caspase-8 in 4T1 tumors following treatment with (A) NVB + 5-FU or (B) NVB + CDDP by western blotting. (C) NF-κB protein levels in 4T1 tumors treated with or NVB + CDDP. (D) Detection of OPN (brown) in 4T1 tumors following treatment with low dose and (E) high dose of NVB + CDDP using immunohistochemical staining. (F) Representative images and (G) analysis of OPN in 4T1 tumors in the NVB + 5-FU treatment group. (H) Analysis and (I) images of Ki67⁺ cells in the blood of tumor metastatic mice after treatment with NVB + CDDP using flow cytometry, as well as the (J) analysis and (K) images after NVB + 5-FU treatment. (L) Detection of Ki67⁺ cells in the lungs of metastatic BALB/c mice treated with NVB + 5-FU. n=3. Scale bar, 20 μm. *P<0.05, **P<0.01 vs. control. 5-FU, fluorouracil; CDDP, cisplatin; Con, control; IOD, integral optical density; ns, not significant; NVB, vinorelbine; OPN, osteopontin; ns, not significant.

in the assessment of cell proliferation rates than the levels in peripheral blood.

Dual-directional effect of NVB combined with CDDP or 5-FU on the apoptosis of endothelial and tumor cells in vitro. To explore the direct effect of NVB combined with CDDP or 5-FU on endothelial and tumor cells, cell viability, apoptosis, migration and invasion rates were assessed *in vitro*. The 50% inhibitory concentration (IC_{50}) of NVB, CDDP and 5-FU were 3.6, 1.1×10^4 and 4.5×10^4 nM for HUVECs, respectively. HUVEC viability was significantly suppressed following treatment with NVB + CDDP [concentrations $\geq 1/8$ of the $C_{\max(NVB + CDDP)}$] and NVB + 5-FU [concentrations $\geq 1/32$ of the $C_{\max(NVB + 5-FU)}$] (Fig. 4A). Meanwhile, HUVEC apoptosis significantly increased by 220.66 and 133.81% (both $P < 0.01$) following exposure to $3.6/1.1 \times 10^4$ nM NVB + CDDP and $3.6/4.5 \times 10^4$ nM NVB + 5-FU, whereas it was inhibited by 32.89 and 28.31% (both $P < 0.05$) following treatment with 0.03/88 nM NVB + CDDP and $0.1/1.4 \times 10^3$ nM NVB + 5-FU, compared with untreated cells (Fig. 4B). In addition, the migration and invasion levels of HUVECs were significantly upregulated by 107.75% ($P < 0.01$) and 40.18% ($P < 0.05$), respectively, following exposure to 0.03/88 nM NVB + CDDP, and by 141.11% ($P < 0.01$) and 46.72% ($P < 0.05$), respectively, following treatment with $0.1/1.4 \times 10^3$ nM NVB + 5-FU, compared with the respective control cells (Fig. 4C and D). However, higher concentrations of $3.6/1.1 \times 10^4$ nM NVB + CDDP or $3.6/4.5 \times 10^4$ nM NVB + 5-FU slightly inhibited migration and invasion, compared with the control cells, but these changes were not statistically significant.

For 4T1 tumor cells, the IC_{50} values of NVB, CDDP and 5-FU were 4, 1.2×10^3 and 340 nM, respectively. NVB + CDDP and NVB + 5-FU had a significant inhibitory effect on cell viability following exposure to concentrations of $\geq 1/4$ of the C_{\max} , and a significant enhancement effect was observed following exposure to $1/32$ of the C_{\max} of NVB + CDDP, compared with the untreated cells (Fig. 4E). The apoptosis levels of 4T1 cells were significantly increased by 40.38 and 61.86% following treatment with 4/1,200 nM NVB + CDDP and 4/340 nM NVB + 5-FU, respectively, but were decreased by 39.74 and 30.41% following treatment with 0.125/37.5 nM NVB + CDDP and 0.06/5.3 nM NVB + 5-FU, respectively, compared with untreated cells (all $P < 0.05$; Fig. 4F). Furthermore, treatment with 0.25/75 nM NVB + CDDP significantly increased migration and invasion by 39.87% ($P < 0.05$) and 73.19% ($P < 0.01$), respectively, and treatment with 0.03/2.7 nM NVB + 5-FU significantly increased migration and invasion by 48.36% ($P < 0.05$) and 88.19% ($P < 0.01$), respectively, compared with the respective controls (Fig. 4G and H). Notably, a high concentration of 4/340 nM NVB + 5-FU increased cell migration and invasion by 65.10 and 28.09% (both $P < 0.05$), compared with untreated cells, and $4/1.2 \times 10^3$ nM NVB + CDDP increased migration by 18.03% ($P < 0.05$), compared with untreated cells, but no marked effect on invasion was observed.

Collectively, the results indicated that low concentration NVB-based combination treatments suppressed the apoptosis of endothelial and tumor cells, and stimulated migration and invasion. Moreover, high concentrations had an antiproliferative and apoptotic effect on both endothelial and tumor cells but induced inconsistent effects on cell migration and invasion.

Dual-directional effect of NVB combined with CDDP or 5-FU on myeloid-derived suppressor cells (MDSCs) and macrophages. MDSCs are regarded as important contributors to immunosuppression of the tumor microenvironment (31). To observe the effect of metronomic NVB-based combination regimens on immune cells, MDSC levels were initially measured in the blood and tumors of mice from the tumor growth model, as well as in the lungs of mice from the tumor metastasis model. It was found that the percentage of $Gr1^+CD11b^+$ MDSCs in the peripheral blood increased by 36.50% ($P < 0.05$) and 77.44% ($P < 0.01$) in the 0.0625/0.1 and 0.125/0.2 mg/kg NVB + CDDP treatment groups, respectively, compared with the control (Fig. 5A). In addition, treatments with 0.0525/3.9375, 0.105/7.875 and 0.21/15.75 mg/kg NVB + 5-FU increased the percentage of $Gr1^+CD11b^+$ MDSCs by 80.59, 90.75 and 83.87% (all $P < 0.01$), respectively, while 0.84/63 mg/kg NVB + 5-FU decreased the percentage of $Gr1^+CD11b^+$ MDSCs by 80.32% ($P < 0.01$), compared with the control (Fig. 5B). In tumor tissues, the levels of $CD11b^+$ MDSCs were higher (71.43%) following treatment with 0.21/15.75 mg/kg NVB + 5-FU, and lower (51.79%) following 0.84/63 mg/kg NVB + 5-FU, compared with those in untreated mice (both $P < 0.01$; Fig. 5C and D). In lung tissues, 0.21/15.75 mg/kg NVB + 5-FU significantly increased the number of $CD11b^+$ MDSCs by 52.00%, and 0.84/63 mg/kg NVB + 5-FU decreased the number of $CD11b^+$ MDSCs by 72.00% (both $P < 0.01$; Fig. 5E and F).

A number of studies have revealed that M2 macrophages are involved in tumor growth and metastasis (32,33). To further explore the potential role of macrophages in tumor growth, the levels of total and M2 macrophages were investigated in 4T1 tumor tissues of BALB/c mice from the tumor growth model. The levels of $F4/80^+$ total and $CD206^+$ M2 macrophages increased following treatment with 0.21/15.75 mg/kg NVB + 5-FU, while the levels decreased following 0.84/63 mg/kg NVB + 5-FU (Fig. 5G).

Collectively, the results of the present study demonstrated a dual-directional action of NVB combined with CDDP or 5-FU on tumor growth and metastasis. Moreover, the dual-directional action induced by the metronomic combination chemotherapy may have been the result of a mutual interaction of several mechanisms rather than any single specific mechanism (Fig. 6).

Discussion

There is a great divide between ideal clinical demands and practical applications in cancer chemotherapy, primarily due to the difficulty in achieving an optimal efficacy-toxicity balance (34). A thorough understanding of the dose-response association of metronomic combination chemotherapy is crucial for the success of this chemotherapeutic strategy. In the present study, a dose-dependent dual-directional pharmacological phenomenon was discovered in 4T1 tumor-bearing BALB/c mice treated with NVB + CDDP and NVB + 5-FU at the regular interval of every other day. The results demonstrated that tumor growth and metastases were stimulated following low-dose treatment and was suppressed following higher doses. A previous study also demonstrated that gemcitabine + CDDP at certain low doses facilitated tumor formation and growth in a xenograft mouse model of melanoma (11). These

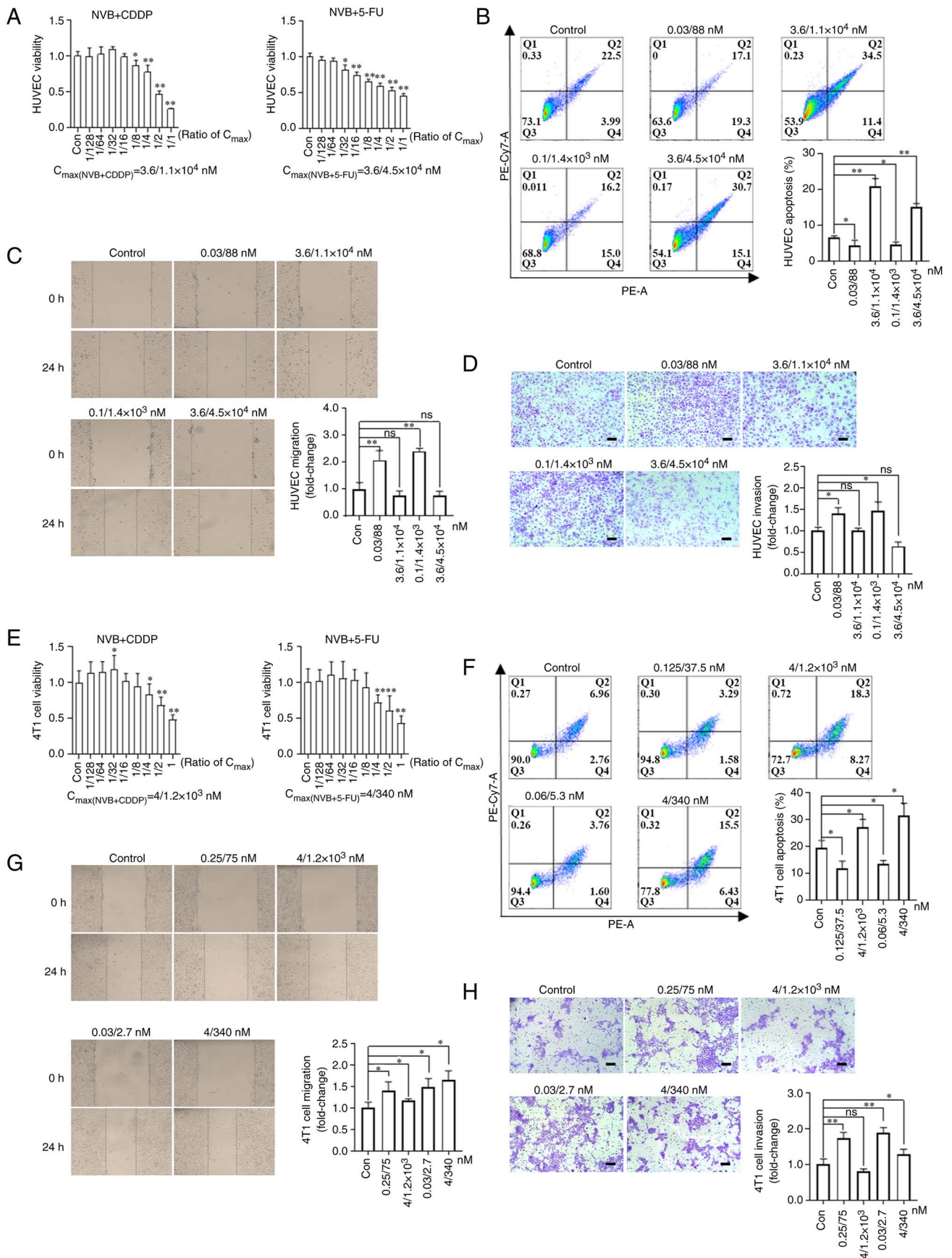


Figure 4. Effects of NVB combined with CDDP or 5-FU on the functions of endothelial and 4T1 tumor cells. (A) Analysis of HUVEC viability following treatment with NVB + CDDP or NVB + 5-FU for 48 h using an MTT assay (n=6). (B) Detection of HUVEC apoptosis induced by NVB + CDDP or NVB + 5-FU by staining with Annexin V-PE and 7-AAD (n=3). HUVEC (C) migration and (D) invasion were investigated following treatment with NVB + CDDP or NVB + 5-FU by wound healing and Transwell assays, respectively (n=3). (E) Cell viability, (F) apoptosis, (G) migration and (H) invasion of 4T1 tumor cells following treatment with NVB + CDDP or NVB + 5-FU. Scale bar, 100 μ m. * $P < 0.05$, ** $P < 0.01$ vs. control. 5-FU, fluorouracil; CDDP, cisplatin; Con, control; HUVEC, human umbilical vein endothelial cell; ns, not significant; NVB, vinorelbine; ns, not significant.

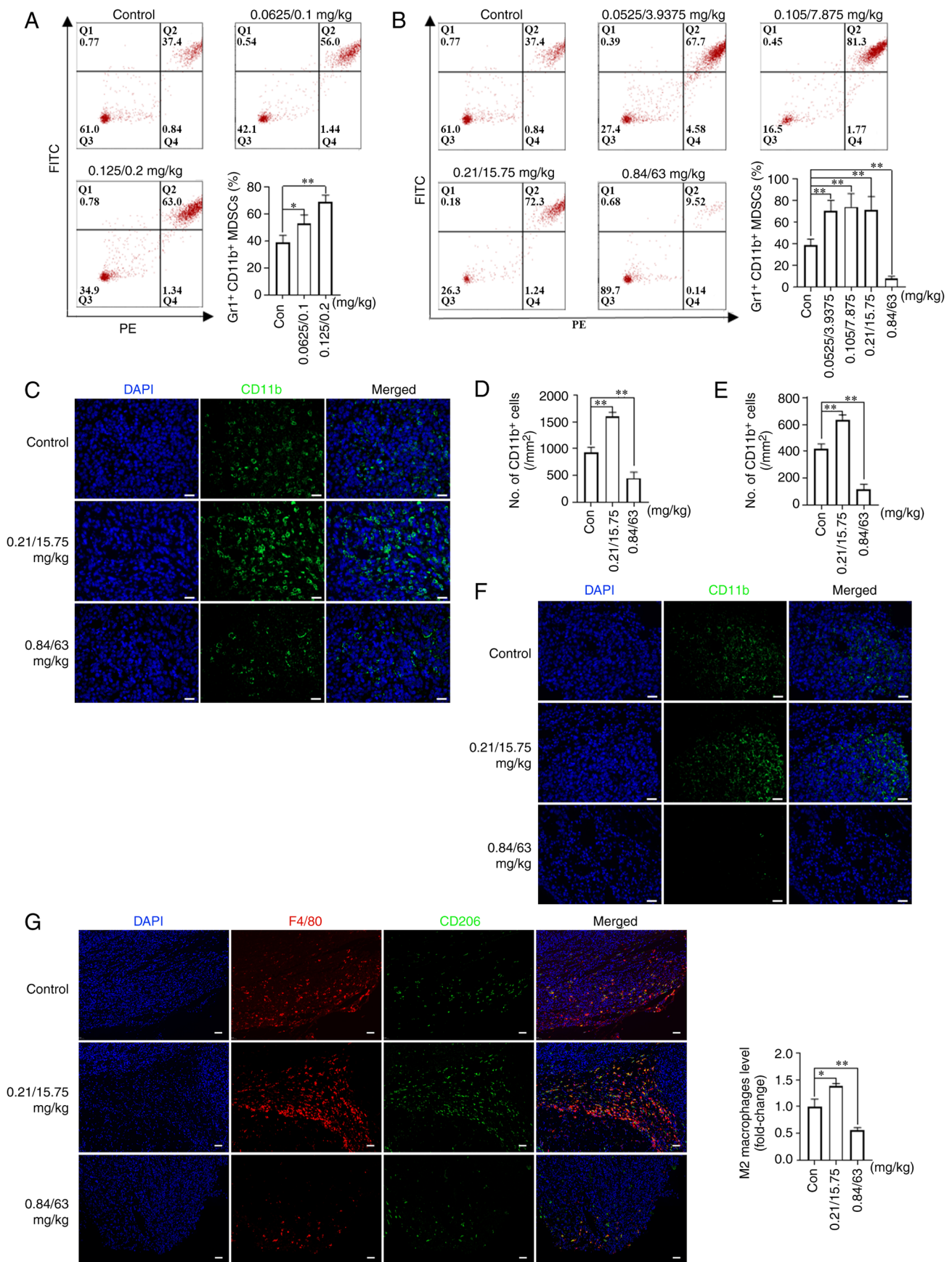


Figure 5. Effects of NVB combined with CDDP or 5-FU on MDSCs and macrophages. The percentage of MDSCs in the peripheral blood of BALB/c mice following treatment with (A) NVB + CDDP or (B) NVB + 5-FU was measured by staining with Gr-1 and CD11b antibodies. (C) Representative images and (D) analysis of CD11b+ MDSCs (green) in the tumors of BALB/c mice treated with NVB + 5-FU using immunofluorescence, as well as the (E) analysis and (F) images in the lungs. (G) Detection of total macrophages (F4/80, red) and M2 macrophages (CD206, green) in tumors treated with NVB + 5-FU. Cell nuclei were counterstained with DAPI (blue) (n=3). Scale bar, 50 μ m. *P<0.05, **P<0.01 vs. control. Gr-1, PE anti-mouse Ly-6G/Ly-6C; 5-FU, fluorouracil; CDDP, cisplatin; Con, control; MDSCs, myeloid-derived suppressor cells; ns, not significant; NVB, vinorelbine.

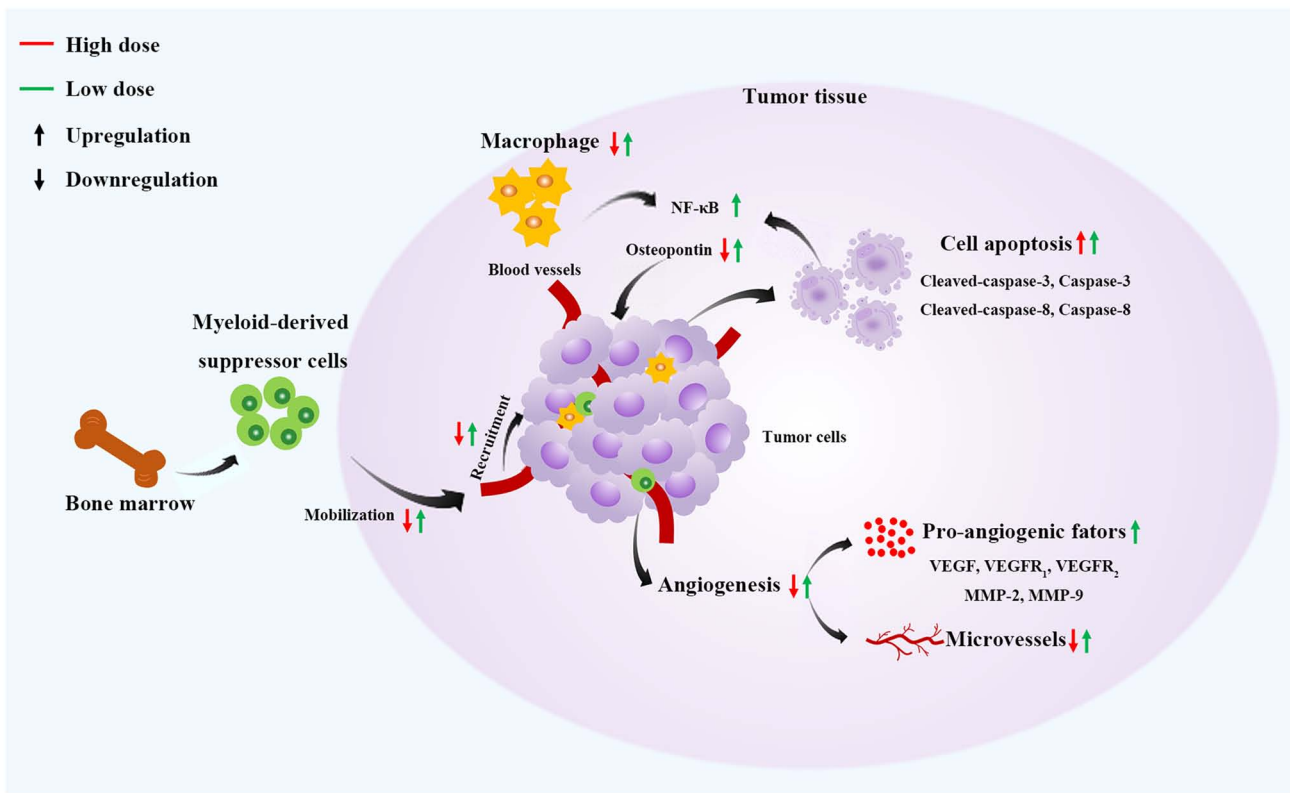


Figure 6. Proposed mechanisms of tumor growth in metronomic combination chemotherapy at different treatment doses of NVB + CDDP or NVB + 5-FU. MMP, matrix metalloproteinase.

results suggested that inappropriate metronomic combination regimens, particularly when empirically determining metronomic regimens, may lead to unexpected outcomes associated with the use of low doses. In addition, the present study demonstrated that the doses that promote or inhibit tumor growth may differ from those that promote or inhibit tumor metastasis in the same drug combination. The modification of antineoplastic agent dosages or their schedules may target different cellular and molecular pathways, but the dosage might be a critical factor in influencing the pharmacological actions of antineoplastic agents administered at the same frequency based on the findings of the present study.

Blood vessels within tumor tissues provide oxygen and nutrients for tumor growth and serve as a route for the circulation of tumor and metastatic cells (35). The results of the present study demonstrated that the level of CD31, a surface marker of neovascular endothelial cells, in tumor or lung tissues increased after the low-dose treatments and decreased after the higher dose treatments, which was in line with the dual-directional effect on tumor growth or metastasis (36). VEGF binding to VEGFR₂ is an important pathway for the functions of endothelial cells and angiogenesis (37). In the present study, western blotting demonstrated that low doses of NVB + CDDP or NVB + 5-FU increased the expression levels of VEGF and VEGFR₂, suggesting that metronomic combination chemotherapy promoted tumor growth by enhancing tumor angiogenesis and the VEGF/VEGFR₂ pathway. VEGFR₁, which is required for metastasis, has an important role in the biological process of angiogenesis (38). The upregulation of VEGFR₁ has been revealed to be associated with

the promotion of tumor angiogenesis and metastasis (11,39). In the present study, low doses of NVB + CDDP or NVB + 5-FU increased the expression of VEGFR₁, suggesting that VEGFR₁ might be an important activator of angiogenesis at low doses of these drugs. However, in the present study, there was no statistically significant reduction in the levels of pro-angiogenic proteins in the high-dose treatments that led to the inhibition of tumor growth, and more research is needed to clarify this aspect. MMPs, including MMP-2 and MMP-9, participate in multiple stages of tumor progression, and are positively correlated with microvessel density and angiogenic markers, such as VEGF (40,41). Tumorigenesis and tumor progression may be mediated by angiogenic processes, such as the increase of vascularization and upregulation of VEGF, MMP-2 and MMP-9 (11,42). The results of the present study demonstrated that the expression levels of MMP-2 and MMP-9 increased in the lungs following low-dose treatments, indicating that angiogenesis participated in the mechanism of promoting tumor metastasis. Unlike conventional chemotherapy targeting fast-dividing tumor cells, endothelial cells responsible for tumor neovascularization have always been regarded as the primary target of MCT (43). In the present study, NVB combined with CDDP or 5-FU suppressed the apoptosis of endothelial cells and stimulated their migration and invasion at low concentrations. However, at higher concentrations, NVB combined with CDDP or 5-FU enhanced apoptosis and suppressed proliferation. These results suggested that the survival and function of endothelial cells directly contributed to the acceleration of tumor growth at low drug doses, while apoptosis and anti-proliferation primarily lead to the inhibition of tumor growth.

Caspase-8 and its downstream protein, caspase-3, are associated with apoptotic machinery and are considered reliable biomarkers for cell apoptosis (44,45). In the present study, high dose NVB + 5-FU increased the expression of pro-apoptotic proteins in tumor tissues, suggesting a positive effect of apoptosis on inhibiting tumor growth. More notably, increased expression of pro-apoptotic proteins was also observed in low-dose treatments that induced the promotion of tumor growth. Emerging evidence has indicated that cell apoptosis could facilitate tumor growth and is correlated with poor prognosis and disease-free survival in certain types of cancer such as breast, head and neck, and colon cancer (46,47). Chang *et al* (28) demonstrated that 5-FU-generated tumor cell debris stimulated tumor growth by triggering the release of OPN from tumor cells in subcutaneous and orthotopic models of colon cancer. In the present study, it was found that the level of OPN increased in low-dose treatments, which indirectly indicated that cell apoptosis may be involved in the promotion of tumor growth mediated by OPN. In addition, cell debris produced by cell death (such as apoptosis and necrosis) promotes tumor growth through the production of pro-inflammation cytokines (48,49). Caspase-3 and caspase-8 have been suggested to stimulate tumor growth through various mechanisms (50). For example, caspase-8 has the non-apoptotic function of promoting the accumulation of NF- κ B and the expression of NF- κ B-dependent cytokines (such as IL-1, IL-8 and VEGF) (45,51,52). Moreover, NF- κ B could also promote angiogenesis by upregulating the signaling pathways involved in angiogenic factors, such as VEGF (53). The results of the present study demonstrated an upregulation of NF- κ B expression following low-dose NVB + CDDP treatment, implying the potential positive action in promotion of tumor growth. However, the role of apoptosis in promoting tumor growth remains unclear and further research is required to elucidate it. In the present study, *in vitro*, low concentrations of NVB + CDDP or NVB + 5-FU suppressed apoptosis and stimulated the migration and invasion of 4T1 tumor cells, which was consistent with the promotion of these functions by low concentrations of gemcitabine + CDDP in B16, MCF-7 and T-47D tumor cells *in vitro* (11). However, the results of 4T1 tumor cells treated with high-concentration NVB combined with CDDP or 5-FU were contradictory, as they revealed that proliferation was inhibited, and apoptosis, migration and invasion were promoted. These results suggested that the anti-apoptosis, migration and invasion of tumor cells might directly stimulate tumor progression, while apoptosis and anti-proliferation contribute to the inhibition of tumor growth.

Clinical data have suggested that MDSCs are strongly correlated with poor overall survival time (54). MDSCs, which can be mobilized into the peripheral blood and recruited to tumor or lung tissues, promote tumor growth and metastasis through angiogenesis, invasion or the formation of pre-metastatic niches (31,55). In a bone marrow transplantation mouse model, it was found that gemcitabine + CDDP treatment promoted the mobilization of Gr1⁺CD11b⁺MDSCs and enhanced the accumulation of bone marrow-derived cells in tumors (11). In the present study, MDSC levels increased in the blood, tumors and lungs of mice following treatment with low-dose NVB + CDDP or NVB + 5-FU, but were decreased following high doses, which suggested that the mobilization and recruitment of MDSCs plays a role in the dual-directional

regulation of tumor growth and metastasis in metronomic combination chemotherapy. In addition to MDSCs, macrophages are another type of immune cell abundantly found in the tumor microenvironment of various solid tumors such as pancreas, breast and lung tumors, and this abundance has been found to be correlated with poor survival time (56). Emerging evidence has revealed that macrophages, specifically M2 macrophages, can promote tumor initiation and progression by enhancing angiogenesis, stimulating tumor cell functions, such as migration, invasion and intravasation, and suppressing antitumor immunity (32). The present study found that both total macrophage and M2 macrophage levels increased in the low-dose NVB + 5-FU group, and decreased in the high-dose group, indicating that macrophages may participate in the dual-directional biological process of tumor growth induced by metronomic combination treatment at different doses. Furthermore, it has been reported that the cross-talk among MDSCs, macrophages and tumor cells affects antitumor immunity by regulating the production of molecules, including IL-6, IL-10, IL-12, TNF- α and NO (57).

In conclusion, the present study illustrated a dual-directional mode of action of NVB-based metronomic combination chemotherapy. The promotion of tumor growth and metastasis induced by low doses of chemotherapeutic drugs highlighted that there is an effective dose interval that varies with different drugs or combinations in metronomic combination chemotherapy. Therefore, more preclinical and clinical studies are needed to optimize specific combined metronomic regimens, including the optimal drug combination, dosage and intervals, prior to their widespread implementation in clinical settings.

Acknowledgements

Not applicable.

Funding

This study was supported by the National Natural Science Foundation of China (grant no. 81372379).

Availability of data and materials

The datasets used and/or analyzed during the current study are available from the corresponding author on reasonable request.

Authors' contributions

HL performed the experiments and wrote the manuscript; ML and JK analyzed the data; YL collected the data; HY interpreted the data and reviewed the work critically for important intellectual content; WF designed and supervised the research. HL, ML, JK and WF confirm the authenticity of all the raw data. All authors read and approved the final version of the manuscript.

Ethics approval and consent to participate

All experiments were approved by The Biomedical Ethics Committee of Xi'an Jiaotong University (Xi'an, China; approval no. 2020-1644).

Patient consent for publication

Not applicable.

Competing interests

The authors declare that they have no competing interests.

References

- Wong HH and Halford S: Dose-limiting toxicity and maximum tolerated dose: Still fit for purpose? *Lancet Oncol* 16: 1287-1288, 2015.
- Gasparini G: Metronomic scheduling: The future of chemotherapy? *Lancet Oncol* 2: 733-740, 2001.
- Pomeroy AE, Schmidt EV, Sorger PK and Palmer AC: Drug independence and the curability of cancer by combination chemotherapy. *Trends Cancer* 8: 915-929, 2022.
- Wu J and Waxman DJ: Immunogenic chemotherapy: Dose and schedule dependence and combination with immunotherapy. *Cancer Lett* 419: 210-221, 2018.
- Chen YL, Chang MC and Cheng WF: Metronomic chemotherapy and immunotherapy in cancer treatment. *Cancer Lett* 400: 282-292, 2017.
- Scharovsky OG, Rico MJ, Mainetti LE, Perroud HA and Rozados VR: Achievements and challenges in the use of metronomics for the treatment of breast cancer. *Biochem Pharmacol* 175: 113909, 2020.
- Cox MC and Bocci G: Metronomic chemotherapy regimens and targeted therapies in non-Hodgkin lymphoma: The best of two worlds. *Cancer Lett* 524: 144-150, 2022.
- Bocci G and Kerbel RS: Pharmacokinetics of metronomic chemotherapy: A neglected but crucial aspect. *Nat Rev Clin Oncol* 13: 659-673, 2016.
- Lien K, Georgsdottir S, Sivanathan L, Chan K and Emmenegger U: Low-dose metronomic chemotherapy: A systematic literature analysis. *Eur J Cancer* 49: 3387-3395, 2013.
- de Ruiter J, Cramer SJ, Smink T and van Putten LM: The facilitation of tumour growth in the lung by cyclophosphamide in artificial and spontaneous metastases models. *Eur J Cancer* 15: 1139-1149, 1979.
- Chen Y, Liu H, Zheng Q, Li H, You H, Feng Y and Feng W: Promotion of tumor progression induced by continuous low-dose administration of antineoplastic agent gemcitabine or gemcitabine combined with cisplatin. *Life Sci* 306: 120826, 2022.
- Dellapasqua S, Bertolini F, Bagnardi V, Campagnoli E, Scarano E, Torrisi R, Shaked Y, Mancuso P, Goldhirsch A, Rocca A, *et al*: Metronomic cyclophosphamide and capecitabine combined with bevacizumab in advanced breast cancer. *J Clin Oncol* 26: 4899-4905, 2008.
- Montagna E, Palazzo A, Maisonneuve P, Canello G, Iorfida M, Sciandivasci A, Esposito A, Cardillo A, Mazza M, Munzone E, *et al*: Safety and efficacy study of metronomic vinorelbine, cyclophosphamide plus capecitabine in metastatic breast cancer: A phase II trial. *Cancer Lett* 400: 276-281, 2017.
- Rossi D: Metronomic oral vinorelbine and lung cancer therapy during the COVID 19 pandemic: A single-center experience. *Lung Cancer* 145: 83-84, 2020.
- Xu B, Sun T, Wang S and Lin Y: Metronomic therapy in advanced breast cancer and NSCLC: Vinorelbine as a paradigm of recent progress. *Expert Rev Anticancer Ther* 21: 71-79, 2021.
- Riesco-Martinez M, Parra K, Saluja R, Francia G and Emmenegger U: Resistance to metronomic chemotherapy and ways to overcome it. *Cancer Lett* 400: 311-318, 2017.
- Munzone E and Colleoni M: Clinical overview of metronomic chemotherapy in breast cancer. *Nat Rev Clin Oncol* 12: 631-644, 2015.
- Romani AMP: Cisplatin in cancer treatment. *Biochem Pharmacol* 206: 115323, 2022.
- Longley DB, Harkin DP and Johnston PG: 5-fluorouracil: Mechanisms of action and clinical strategies. *Nat Rev Cancer* 3: 330-338, 2003.
- National Research Council Committee for the Update of the Guide for the Care and Use of Laboratory Animals: The National Academies Collection: Reports funded by National Institutes of Health. In: *Guide for the Care and Use of Laboratory Animals*. National Academy of Sciences, National Academies Press, Washington, DC, 2011.
- Aston WJ, Hope DE, Nowak AK, Robinson BW, Lake RA and Lesterhuis WJ: A systematic investigation of the maximum tolerated dose of cytotoxic chemotherapy with and without supportive care in mice. *BMC Cancer* 17: 684, 2017.
- Saif MW and von Borstel R: 5-Fluorouracil dose escalation enabled with PN401 (triacetylluridine): Toxicity reduction and increased antitumor activity in mice. *Cancer Chemother Pharmacol* 58: 136-142, 2006.
- Navari RM and Aapro M: Antiemetic prophylaxis for chemotherapy-induced nausea and vomiting. *N Engl J Med* 374: 1356-1367, 2016.
- Xu Y, Ye S, Zhang N, Zheng S, Liu H, Zhou K, Wang L, Cao Y, Sun P and Wang T: The FTO/miR-181b-3p/ARL5B signaling pathway regulates cell migration and invasion in breast cancer. *Cancer Commun (Lond)* 40: 484-500, 2020.
- Magaki S, Hojat SA, Wei B, So A and Yong WH: An introduction to the performance of immunohistochemistry. *Methods Mol Biol* 1897: 289-298, 2019.
- Zhang S, Liu Y, Xiang D, Yang J, Liu D, Ren X and Zhang C: Assessment of dose-response relationship of 5-fluorouracil to murine intestinal injury. *Biomed Pharmacother* 106: 910-916, 2018.
- Deng J, Yang H, Haak VM, Yang J, Kipper FC, Barksdale C, Hwang SH, Gartung A, Bielenberg DR, Subbian S, *et al*: Eicosanoid regulation of debris-stimulated metastasis. *Proc Natl Acad Sci USA* 118: e2107771118, 2021.
- Chang J, Bhasin SS, Bielenberg DR, Sukhatme VP, Bhasin M, Huang S, Kieran MW and Panigrahy D: Chemotherapy-generated cell debris stimulates colon carcinoma tumor growth via osteopontin. *FASEB J* 33: 114-125, 2019.
- Yin Y, Zeng K, Wu M, Ding Y, Zhao M and Chen Q: The levels of Ki-67 positive are positively associated with lymph node metastasis in invasive ductal breast cancer. *Cell Biochemistry Biophysics* 70: 1145-1151, 2014.
- Bruey JM, Kantarjian H, Estrov Z, Zhang Z, Ma W, Albitar F, Abdool A, Thomas D, Yeh C, O'Brien S and Albitar M: Circulating Ki-67 protein in plasma as a biomarker and prognostic indicator of acute lymphoblastic leukemia. *Leuk Res* 34: 173-176, 2010.
- Safarzadeh E, Orangi M, Mohammadi H, Babaie F and Baradaran B: Myeloid-derived suppressor cells: Important contributors to tumor progression and metastasis. *J Cell Physiol* 233: 3024-3036, 2018.
- Cassetta L and Pollard JW: Targeting macrophages: Therapeutic approaches in cancer. *Nature reviews Drug Discovery* 17: 887-904, 2018.
- Chen Y, Zhang S, Wang Q and Zhang X: Tumor-recruited M2 macrophages promote gastric and breast cancer metastasis via M2 macrophage-secreted CHI3L1 protein. *J Hematol Oncol* 10: 36, 2017.
- Barbolosi D, Ciccolini J, Lacarelle B, Barlési F and André N: Computational oncology-mathematical modelling of drug regimens for precision medicine. *Nat Rev Clin Oncol* 13: 242-254, 2016.
- Ebos JM and Kerbel RS: Antiangiogenic therapy: Impact on invasion, disease progression, and metastasis. *Nat Rev Clin Oncol* 8: 210-221, 2011.
- Zhang T, Zhang L, Gao Y, Wang Y, Liu Y, Zhang H, Wang Q, Hu F, Li J, Tan J, *et al*: Role of aneuploid circulating tumor cells and CD31⁺ circulating tumor endothelial cells in predicting and monitoring anti-angiogenic therapy efficacy in advanced NSCLC. *Mol Oncol* 15: 2891-2909, 2021.
- Chatterjee S, Heukamp LC, Siobal M, Schöttle J, Wieczorek C, Peifer M, Frasca D, Koker M, König K, Meder L, *et al*: Tumor VEGF:VEGFR2 autocrine feed-forward loop triggers angiogenesis in lung cancer. *J Clin Invest* 123: 1732-1740, 2013.
- Freire Valls A, Knipper K, Giannakouri E, Sarachaga V, Hinterkopf S, Wuehrl M, Shen Y, Radhakrishnan P, Klose J, Ulrich A, *et al*: VEGFR1⁺ Metastasis-associated macrophages contribute to metastatic angiogenesis and influence colorectal cancer patient outcome. *Clin Cancer Res* 25: 5674-5685, 2019.
- Liu W, Xu J, Wang M, Wang Q, Bi Y and Han M: Tumor-derived vascular endothelial growth factor (VEGF)-a facilitates tumor metastasis through the VEGF-VEGFR1 signaling pathway. *Int J Oncol* 39: 1213-1220, 2011.
- Riedel F, Götte K, Schwalb J, Bergler W and Hörmann K: Expression of 92-kDa type IV collagenase correlates with angiogenic markers and poor survival in head and neck squamous cell carcinoma. *Int J Oncol* 17: 1099-1105, 2000.
- Kessenbrock K, Plaks V and Werb Z: Matrix metalloproteinases: Regulators of the tumor microenvironment. *Cell* 141: 52-67, 2010.

42. Thaker PH, Han LY, Kamat AA, Arevalo JM, Takahashi R, Lu C, Jennings NB, Armaiz-Pena G, Bankson JA, Ravoori M, *et al*: Chronic stress promotes tumor growth and angiogenesis in a mouse model of ovarian carcinoma. *Nat Med* 12: 939-944, 2006.
43. Browder T, Butterfield CE, Kräling BM, Shi B, Marshall B, O'Reilly MS and Folkman J: Antiangiogenic scheduling of chemotherapy improves efficacy against experimental drug-resistant cancer. *Cancer Res* 60: 1878-1886, 2000.
44. Silva F, Padin-Iruegas ME, Caponio VCA, Lorenzo-Pouso AI, Saavedra-Nieves P, Chamorro-Petronacci CM, Suarez-Penaranda J and Perez-Sayans M: Caspase 3 and cleaved Caspase 3 expression in tumorigenesis and its correlations with prognosis in head and neck cancer: A systematic review and meta-analysis. *Int J Mol Sci* 23: 11937, 2022.
45. Tummers B and Green DR: Caspase-8: regulating life and death. *Immunol Rev* 277: 76-89, 2017.
46. Haak VM, Huang S and Panigrahy D: Debris-stimulated tumor growth: A Pandora's box? *Cancer Metastasis Rev* 40: 791-801, 2021.
47. Huang JS, Yang CM, Wang JS, Liou HH, Hsieh IC, Li GC, Huang SJ, Shu CW, Fu TY, Lin YC, *et al*: Caspase-3 expression in tumorigenesis and prognosis of buccal mucosa squamous cell carcinoma. *Oncotarget* 8: 84237-84247, 2017.
48. Weigert A, Mora J, Sekar D, Syed S and Brüne B: Killing is not enough: How apoptosis hijacks tumor-associated macrophages to promote cancer progression. *Adv Exp Med Biol* 930: 205-239, 2016.
49. Revesz L: Effect of tumour cells killed by x-rays upon the growth of admixed viable cells. *Nature* 178: 1391-1392, 1956.
50. Donato AL, Huang Q, Liu X, Li F, Zimmerman MA and Li CY: Caspase 3 promotes surviving melanoma tumor cell growth after cytotoxic therapy. *J Invest Dermatol* 134: 1686-1692, 2014.
51. Fritsch M, Günther SD, Schwarzer R, Albert MC, Schorn F, Werthenbach JP, Schiffmann LM, Stair N, Stocks H, Seeger JM, *et al*: Caspase-8 is the molecular switch for apoptosis, necroptosis and pyroptosis. *Nature* 575: 683-687, 2019.
52. Fianco G, Contadini C, Ferri A, Cirotti C, Stagni V and Barilà D: Caspase-8: A novel target to overcome resistance to chemotherapy in glioblastoma. *Int J Mol Sci* 19: 3798, 2018.
53. Zhu CC, Chen C, Xu ZQ, Zhao JK, Ou BC, Sun J, Zheng MH, Zong YP and Lu AG: CCR6 promotes tumor angiogenesis via the AKT/NF- κ B/VEGF pathway in colorectal cancer. *Biochim Biophys Acta Mol Basis Dis* 1864: 387-397, 2018.
54. Lang S, Bruderek K, Kaspar C, Höing B, Kanaan O, Dominas N, Hussain T, Droegge F, Eyth C, Hadaschik B and Brandau S: Clinical relevance and suppressive capacity of human Myeloid-derived suppressor cell subsets. *Clin Cancer Res* 24: 4834-4844, 2018.
55. Udumula MP, Sakr S, Dar S, Alvero AB, Ali-Fehmi R, Abdulfatah E, Li J, Jiang J, Tang A, Buckers T, *et al*: Ovarian cancer modulates the immunosuppressive function of CD11b⁺Gr1⁺ myeloid cells via glutamine metabolism. *Mol Metab* 53: 101272, 2021.
56. Nielsen SR and Schmid MC: Macrophages as Key drivers of cancer progression and metastasis. *Mediators Inflamm* 2017: 9624760, 2017.
57. Beury DW, Parker KH, Nyandjo M, Sinha P, Carter KA and Ostrand-Rosenberg S: Cross-talk among myeloid-derived suppressor cells, macrophages, and tumor cells impacts the inflammatory milieu of solid tumors. *J Leukoc Biol* 96: 1109-1118, 2014.



Copyright © 2023 Liu et al. This work is licensed under a Creative Commons Attribution-NonCommercial-NoDerivatives 4.0 International (CC BY-NC-ND 4.0) License.